

## Mesoscopic Effects in the Quantum Hall Regime

R. N. Bhatt and Xin Wan\*

Department of Electrical Engineering, Princeton University, Princeton, NJ 08544-5263, USA

**Abstract.** We report results of a study of (integer) quantum Hall transitions in a single or multiple Landau levels for non-interacting electrons in disordered two-dimensional systems, obtained by projecting a tight-binding Hamiltonian to corresponding magnetic subbands. In finite-size systems, we find that mesoscopic effects often dominate, leading to apparent non-universal scaling behaviour in higher Landau levels. This is because localization length, which grows exponentially with Landau level index, exceeds the system sizes amenable to numerical study at present. When band mixing between multiple Landau levels is present, mesoscopic effects cause a crossover from a sequence of quantum Hall transitions for weak disorder to classical behaviour for strong disorder. This behaviour may be of relevance to experimentally observed transitions between quantum Hall states and the insulating phase at low magnetic fields.

**Keywords.** mesoscopic effects, quantum Hall transitions, finite-size scaling

**PACS Nos** 73.43.Cd, 73.43.Nq, 71.30.+h

### 1. Introduction

One of the central ideas used to analyse phase transitions between different integer quantum Hall states in two-dimensional electron systems is finite size scaling. Transitions between plateaus in the Hall conductivity are characterized by a localization length  $\xi$  which diverges at the critical point  $s_c$ ,  $\xi(s) \sim |s - s_c|^{-\nu}$ .  $s$  can be energy  $E$  (in numerical calculations), or magnetic field  $B$  (in experiments). Finite size scaling asserts that various quantities for a finite system of size  $L$  will depend on the ratio  $L/\xi$ . (In experiments, the relevant size is the dephasing length, which is determined by temperature  $T$  through inelastic scattering mechanisms). Thus, a system realizes its finite size when  $L/\xi \leq 1$ , when singularities associated with the phase transition are cut off by the finite size. This defines the range where finite-size effects become important. Therefore, long length scales always pose a challenge for numerical calculations, in which the system size is limited by the current computing power. Unfortunately, the integer quantum Hall transitions in higher Landau levels are among such cases.

---

\*Present address: National High Magnetic Field Laboratory, Florida State University, Tallahassee, FL 32310, USA

To a large extent, the difficulties of identifying the nature of the quantum Hall transitions in weak magnetic fields come from the same origin. In this case, the mixing of neighbouring Landau levels exacerbates the situation even further. According to the global phase diagram, developed by early theoretical efforts [], for integer quantum Hall transitions, the Hall conductance can only change by  $e^2/h$  at the transitions, whether in high magnetic fields or in low fields. Early experiments [] were consistent with this expectation (counting spin degeneracy). However, more recent experiments by Song *et al.* [], Hilke *et al.* [], and Kravchenko *et al.* [] cast doubts on the global phase diagram, as their data were interpreted as showing direct transitions from an integer quantum Hall state with Hall conductance  $ne^2/h$  ( $n > 1$ ) to an insulator. Subsequently, some numerical calculations [] appeared to corroborate the existence of direct transitions between quantum Hall liquids with Hall conductance of  $ne^2/h$  ( $n > 1$ ) to the low field insulator. However, it has never become clear whether such “transitions” are true quantum phase transitions or merely the manifestation of consecutive transitions which are too close to resolve.

In this paper, we discuss the mesoscopic effects in the quantum Hall regime, in particular the effects of long length scales on the scaling behaviour and on the low-field transitions, using a tight-binding lattice model of two-dimensional non-interacting electrons in a random potential and a perpendicular magnetic field. We describe our model with truncated Hilbert space and various methods in Sec. 2. and 3. respectively. Section 4. contains the discussions on the difference of the scaling behaviour in Landau levels with increasing index, as a result of the increasing length scales. We then turn to transitions at low magnetic fields in Sec. 5., before summarizing our results and conclusions in Sec. 6.

## 2. Model

We consider a tight-binding Hamiltonian of non-interacting electrons on a two-dimensional square lattice with nearest neighbour hopping, subject to a uniform perpendicular magnetic field  $\mathbf{B}$ :

$$H = -t \sum_{\langle ij \rangle} (e^{i\theta_{ij}} c_i^\dagger c_j + h.c.) + \sum_i \epsilon_i c_i^\dagger c_i. \quad (1)$$

$\epsilon_i$  are the on-site random potentials, and the magnitude of the hopping matrix element  $t = 1$  is chosen as the unit of energy for convenience. As a consequence of the perpendicular magnetic field  $\mathbf{B}$ , there is a magnetic flux  $\phi$  per unit cell given by

$$\frac{\phi}{\phi_0} = \frac{eBa_0^2}{hc} = \frac{1}{2\pi} \sum_{\square} \theta_{ij}, \quad (2)$$

where  $\phi_0 = hc/e$  is the magnetic flux quantum, and  $a_0$  is the lattice constant. The random potential  $\epsilon_i$ , are taken to be *independent* random variables, chosen from an identical distribution (so ensemble averaged quantities are translationally invariant). We consider two specific distributions:

- (i) a rectangular box (i.e. uniform) distribution on  $[-W, W]$ ,

$$P(\epsilon) = \begin{cases} \frac{1}{2W}, & -W \leq \epsilon \leq W, \\ 0, & \text{otherwise,} \end{cases} \quad (3)$$

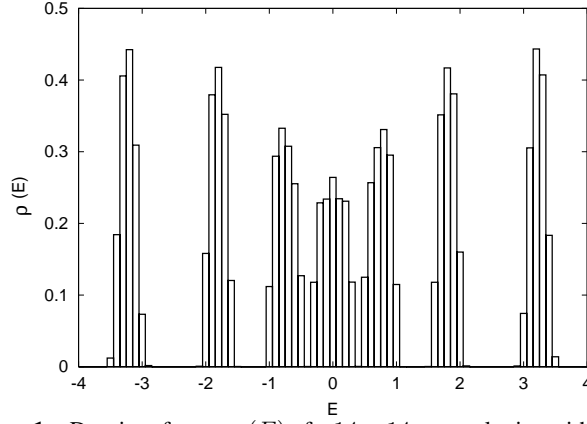


**Figure 1.** Density of states  $\rho(E)$  of a  $14 \times 14$  square lattice with magnetic flux  $\phi_0/7$  per unit cell and  $W = 0.5$  rectangular box distributed disorder.

(ii) a Gaussian distribution with standard deviation  $\sigma$ ,

$$P(\epsilon) = \frac{1}{\sqrt{2\pi}\sigma} \exp\left(-\frac{\epsilon^2}{2\sigma^2}\right). \quad (4)$$

The calculation of the energy spectrum can be done for rational  $\phi/\phi_0 = p/q$ , where  $p$  and  $q$  are integers, chosen to have no common factors. The whole spectrum [] is commonly known as the Hofstadter butterfly, so named because of the butterfly-like self-similar pattern in terms of the parameter  $\phi$ . For each pair of  $p$  and  $q$ , in the absence of disorder, the original tight-binding band is split into  $q$  magnetic subbands; these are then broadened by disorder. Figure 1 shows the density of states of a 14 by 14 square lattice with magnetic flux  $\phi_0/7$  per unit cell. The seven magnetic subbands are well separated by energy gaps at disorder strength  $W = 0.5$ .

The Hall conductance of *each* of the  $q$  magnetic subbands, when they are separated by energy gaps, has been shown to be quantized []. The Hall conductance  $\sigma_r$  (in units of  $e^2/h$ ), when the lowest  $r$  subbands are occupied, is related to  $p$  and  $q$  by a Diophantine equation [],  $r = qs_r + p\sigma_r$ , where  $s_r$  is an integer chosen such that  $|\sigma_r| \leq q/2$ . The quantized Hall conductance has a topological origin, which is the Chern number of a fiber bundle defined by the magnetic Bloch wavefunctions on the torus, the magnetic Brillouin zone. For the case of  $p = 1$  and  $q > 1$  an odd integer, each of the  $(q - 1)$  side subbands carries Hall conductance  $e^2/h$ . The center subband, on the other hand, has Hall conductance of  $-(q - 1)e^2/h$ , guaranteeing that the total Hall conductance of all the subbands of the tight-binding system is zero. The continuum model is achieved in the limit  $q \rightarrow \infty$ , where each of the side subbands corresponds to a Landau level, while the center subband, with no counterpart in the continuum model, is mapped to infinite energy. For finite  $q$ , it is expected that the side subbands near the edges of the spectrum, correspond closely to the Landau levels in the continuum model.

Just like in the continuum model [], we can project the Hamiltonian to a subspace spanned by the eigenstates in the subbands of interest, obtaining from diagonalizing the tight-binding Hamiltonian in the absence of disorder. This truncation process is equivalent

to the addition of a pseudopotential that pushes the subbands not of interest to positive or negative infinite energy. The projection can be easily justified in the strong field limit (weak disorder), where there are energy gaps separating the subbands. On the other hand, in the case of weak magnetic fields (strong disorder), numerical calculations show that the center subband widens with increasing disorder [] and the negative Hall conductance carried by the central subband neutralizes the Hall conductance of the opposite sign carried by side subbands. This has been interpreted as quantum phase transitions from the quantum Hall liquids (with arbitrary integer filling factors) to the insulating state []. However, since there is no center subband in the continuum model, we have chosen to work with a projected Hamiltonian in a truncated Hilbert space with multiple side subbands only. This has a major advantage that unphysical effects due to the center subband in the discrete lattice model are avoided. (We note that the actual experimental system is on a discrete lattice, but that is on an atomic scale, while the physics we are concerned with is on the scale of the magnetic length, which is two orders of magnitude larger). We believe the projected Hamiltonian should keep the essential features of the low magnetic field physics, at least near the bottom of the spectrum where interactions with truncated higher Landau levels are weak.

### 3. Chern Number and Thouless Number

We consider a system of size  $L_x \times L_y$  with generalized periodic boundary condition

$$t(\mathbf{L}_{x,y})|m\rangle = e^{i\theta_{x,y}}|m\rangle \quad (5)$$

where  $t(\mathbf{L}_{x,y})$  is the magnetic translation operator in x or y direction. The Hall conductance of an eigenstate can be calculated by the Kubo formula as []

$$\sigma_{xy}(m; \theta_x, \theta_y) = \frac{ie^2\hbar}{L_x L_y} \sum_{n \neq m} \frac{\langle m|v_x|n\rangle \langle n|v_y|m\rangle - h.c.}{(E_n - E_m)^2}. \quad (6)$$

Here  $|m\rangle, |n\rangle$  are eigenstates for the boundary condition Eq. (5) and  $v_x, v_y$  are components of the velocity operator. Thouless *et al.* showed that the averaged Hall conductance can be written as a quantized integral []

$$\sigma_{xy}(m) \equiv \frac{1}{(2\pi)^2} \int d\theta_x d\theta_y \sigma_{xy}(m; \theta_x, \theta_y) = C(m) \frac{e^2}{h}, \quad (7)$$

where  $C(m)$  is an integer, known as the Chern number of the eigenstate. States with non-zero Chern number conduct Hall current and can be identified as conducting states []. The total Hall conductance  $\sigma_{xy}(E_f)$  for a given position of the Fermi level  $E_f$  is obtained by summing over the Hall conductances of the filled states.

The longitudinal conductivity  $\sigma_{xx}$ , related to Thouless number, may also be used to distinguish extended states from localized states []. Thouless number, which describes the sensitivity of an eigenstate to the change in boundary conditions, is defined in dimensionless form [] by the equation:

$$g_L(E) = \frac{\langle \delta E \rangle}{\langle \Delta E \rangle} \sim \frac{h}{e^2} \sigma_{xx}, \quad (8)$$

where  $\langle \delta E \rangle$  is the average shift in the energy level due to a change of boundary condition from periodic to anti-periodic, and  $\langle \Delta E \rangle = 1/L^2 \rho_L(E)$  the mean energy level separation. In second-order perturbation theory, the change in eigenenergy is proportional to the longitudinal conductance []; the proportionality constant is of the order of unity, with a precise value that depends on the exact definition of the energy shift  $\langle \delta E \rangle$ .

As the size of the system increases, the Thouless number in the localized regime decreases, while at the critical point the Thouless number goes to a universal value. In the scaling regime, the dimensionless quantity depends on system size only through the ratio  $L/\xi(E)$ :

$$g_L(E) = \tilde{g}(L/\xi) = g(L^{1/\nu}|E - E_c|), \quad (9)$$

where the localization length  $\xi$  diverges at the critical energy  $E_c$ , in a power law fashion,

$$\xi(E) \sim |E - E_c|^{-\nu}. \quad (10)$$

We define the width of a Thouless number curve  $g_L(E)$  as

$$W(L) = \frac{1}{W_{\text{DOS}}(L)} \left[ \frac{\int_{-\infty}^{\infty} (E - E_c)^2 g_L(E) dE}{\int_{-\infty}^{\infty} g_L(E) dE} \right]^{1/2}. \quad (11)$$

$W(L)$  is normalized by  $W_{\text{DOS}}(L)$ , the width of the corresponding density-of-states  $\rho_L(E)$ ,

$$W_{\text{DOS}}(L) = \left[ \frac{\int_{-\infty}^{\infty} (E - E_c)^2 \rho_L(E) dE}{\int_{-\infty}^{\infty} \rho_L(E) dE} \right]^{1/2}, \quad (12)$$

which is expected to be only very weakly dependent on  $L$ . Using Eq. (10), the width of a Thouless number curve can be shown to vary with system size as a power law:

$$W(L) \sim L^{-1/\nu}. \quad (13)$$

Alternatively, we may compute the area  $A(L)$  under  $g_L(E)$ , as  $A(L) = \int_{-\infty}^{\infty} g_L(E) dE$ . In the scaling regime, we have

$$A(L) \sim L^{-1/\nu} \quad (14)$$

with the same exponent  $\nu$ .

## 4. Quantum Hall Transitions in a Single Subband

### 4.1 The lowest subband

We start with the simplest case - truncation of the Hilbert space to the lowest subband, which we compare with the numerous results in the lowest Landau level available to date. The critical behaviour of the quantum Hall transition in the lowest Landau level has been studied numerically by various groups []. Numerical results in different models agree that

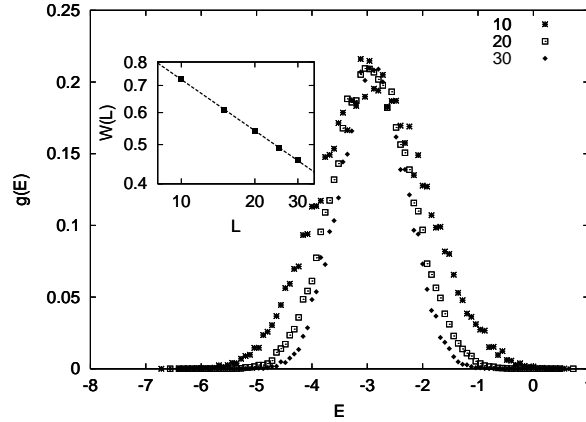


**Figure 2.** Thouless number  $g(E)$  of the lowest subband with  $W/t = 5$  for  $10 \times 10$ ,  $20 \times 20$ , and  $30 \times 30$  lattices. The inset shows the normalized width of  $g(E)$  as a function of size  $L$ , on a log-log scale.

the localization length diverges with critical exponent  $\nu \simeq 2.35 \pm 0.1$  in the vicinity of the critical energy  $E_c$  at the band center. In particular, Huo and Bhatt found the localization length critical exponent  $\nu = 2.4 \pm 0.1$ , obtained from the finite-size scaling of the density of extended states identified by a Chern number calculation [1].

If we choose  $\phi/\phi_0 = 1/5$ , the tight-binding band splits into five magnetic subbands, which carry Hall conductance of 1, 1, -4, 1, 1, in units of  $e^2/h$ , respectively. We separate the lowest subband carrying Hall conductance  $e^2/h$  from the rest of the four subbands (carrying total Hall conductance  $-e^2/h$ ) by truncating the Hilbert space as described above. We studied systems with size  $L = 10, 15, 20, 25$  and  $30$ , with a rectangular box distributed random potential  $W/t = 5$ . We diagonalized between 200 and 1,800 samples with different random potential configurations from the ensemble, for calculating average quantities, depending on size. Figure 2 shows the Thouless number of the edge subband for sizes  $L = 10, 20$  and  $30$ . We clearly see the shrinkage of the width of the Thouless number as the system size increases. Meanwhile, the peak value of the Thouless number for different sizes remains fixed around  $g_0 \simeq 0.21$ , which helps us locate the critical energy  $E_c = -2.9$ . The width of Thouless number of different sizes calculated by Eq. (11) (and normalized by the width of the density-of-states), is plotted in the inset on a log-log scale. Fitting the width to a straight line (a power law), we can extract the localization length exponent  $\nu = 2.4 \pm 0.1$  according to Eq. (13), which agrees with the exponent found for the lowest Landau level in the continuum model. The finite-size scaling fit suggests that in the thermodynamic limit ( $L \rightarrow \infty$ ) the Thouless number, or the longitudinal conductance  $\sigma_{xx}$ , vanishes everywhere except at one single energy  $E_c$ , where the localization length diverges. This demonstrates that, under truncation, the edge subband has the same scaling behaviour as the lowest Landau level.

In order to test the universality of the scaling behaviour, we studied systems with various values of magnetic flux per unit cell, including  $\phi/\phi_0 = 1/3, 1/5, 1/6, 1/7$ , and  $1/9$ , choosing either rectangular box distributed or Gaussian distributed potential, with disorder strength  $W/t$  (or  $\sigma/t$ ) varying from 1 to  $\infty$  ( $t \rightarrow 0$ ). We calculated the Thouless number of the truncated lowest magnetic subband of these systems up to  $L = 66$  and averaged

over as many as 100,000 random potential realizations (for  $L = 3$ ). With these choices of system configurations, we found the localization length critical exponent  $\nu = 2.3 \pm 0.2$ , obtained from the finite-size scaling of the width of the Thouless number. The peak value  $g_0$  of the Thouless number was found for all different cases to be  $g_0 = 0.21 \pm 0.02$ . This indicates that  $\nu$  and  $g_0$  are universal in the scaling regime, which includes system sizes as small as  $L = 10$  in most cases.

#### 4.2 The second lowest subband

It has been recognized that the localization length,

$$\xi = \xi_0 \left| \frac{E - E_c}{\Delta E} \right|^{-\nu}, \quad (15)$$

in higher Landau levels is much larger than that in the lowest Landau level []. In the above equation,  $\Delta E$  is the width of the density of states  $\rho(E)$ .  $\xi_0$ , the  $E$ -independent prefactor, is distinct for each Landau level, and is of order of the lattice constant in the lowest Landau level. The localization length in higher Landau levels grows rapidly with increasing Landau level number (exponentially as its square in simple approximations), raising great difficulties in numerical calculation of the critical exponent in higher Landau levels. This difficulty has been reflected, in particular from the observation of non-universal (larger-than-expected) exponent, in early works []. The universal scaling behaviour can, therefore, only be restored in much larger systems, unless the localization length can be reduced.

A potential with a non-zero correlation length is known to be able to reduce the localization length substantially, to a numerically acceptable value. Calculations for the second lowest Landau level suggest that the value of the localization length exponent  $\nu$  depends on the correlation length  $l$  of the random potential []. Mieczkowski showed that  $\nu$  decreases from 6.2 for  $l = 0$  to 2.3 for  $l = 4l_c$ , where  $l_c = (\hbar c/eB)^{1/2}$  is the magnetic length []. Huckestein also obtained for a correlation length  $l = l_c$  the same scaling behaviour as in the lowest Landau level []. We found very similar behaviour in the truncated second lowest magnetic subband, which, again, shows the correspondence between our lattice model with the truncated Hilbert space and the continuum model.

In our lattice model, a correlated potential is generated as follows. First, generate an uncorrelated random potential  $\epsilon_i^0$  with the desired distribution. We then introduce correlation between random potential on different sites by defining

$$\epsilon_i = \frac{\sum_j \epsilon_j^0 e^{-d_{ij}^2/l^2}}{\sum_j e^{-d_{ij}^2/l^2}}, \quad (16)$$

where  $d_{ij}$  is the distance between sites  $i$  and  $j$ . The correlation function between the two sites

$$\langle \epsilon_i \epsilon_j \rangle \sim e^{-d_{ij}^2/l^2}, \quad (17)$$

with correlation length  $l$ . It should be emphasized that our correlated potentials have Gaussian correlation; to get an exponential correlation, an appropriate modification of Eq. (16) is necessary.

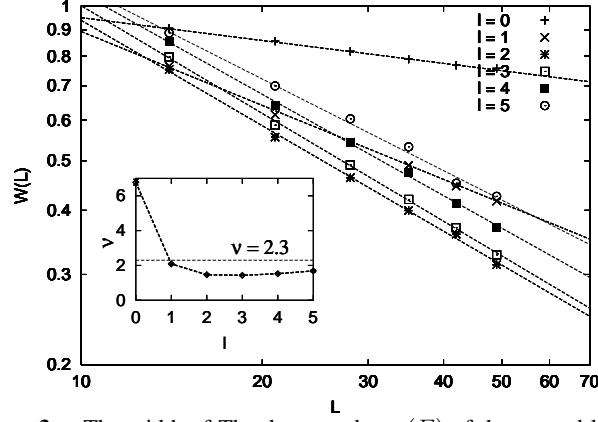


**Figure 3.** The width of Thouless number  $g(E)$  of the second lowest subband as a function of size  $L$  on a log-log scale. The inset shows the localization length critical exponent  $\nu$  calculated from the slopes of the different lines in main figure for different correlation lengths  $l$ .

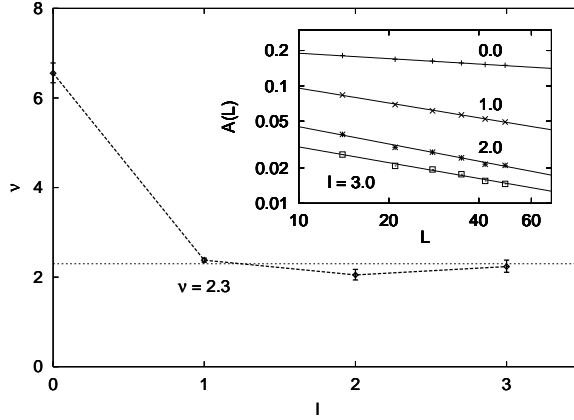
In this section, we study the Thouless number of the (truncated) second lowest subband, of a seven-subband system ( $\phi/\phi_0 = 1/7$ ), with correlated potential generated using a rectangular box distribution for  $\epsilon_i$ . After projection we set  $t = 0$  (infinite disorder limit) to reduce finite size effects. For sizes  $L = 14$  to  $49$ , we diagonalized  $150 - 1,800$  samples, depending on  $L$ . We calculated the Thouless number  $g(E)$  of the subband with various correlation lengths. Figure 3 summarizes the width of the  $g(E)$  normalized by the width of the density of states. On the double logarithmic plot, the width versus size follows straight lines apparently consistent with the scaling hypothesis Eq. (13). However, the localization length critical exponent  $\nu$  extracted from the slope of the curves is not universal. The inset of Fig. 3 shows that  $\nu$  decreases from  $6.8$  with  $l = 0$  to  $1.4$  with  $l = 3$ , and then increases slowly to  $1.7$  with  $l = 5$ . This curve is very similar to the one obtained by Guo [] in the study of the critical behaviour in the first Landau level in the continuum model. The curve crosses the expected universal exponent  $\nu = 2.3$  for  $l \simeq 1$ .

Figure 3 also shows that  $W(L)$  is minimized with  $l = 2$ , suggesting that the localization length is reduced with increasing correlation length  $l$  of the correlated potential, at least for  $l \leq 2$ . However, with  $l = 2$ ,  $\nu = 1.5$  is much smaller than the expected  $\nu = 2.3$ . This suggests that the random correlated potential introduces an irrelevant length scale  $\zeta$ , which depends on the correlation length  $l$ , so that

$$g_L(E) = \tilde{g} \left( \frac{L}{\xi}, \frac{L}{\zeta} \right), \quad (18)$$

Only when  $L, \xi \gg \zeta$  can we restore the universal behaviour of quantum Hall transitions. Due to this additional length scale  $\zeta$ , Thouless number, in general, does not have either the universal functional form or the universal peak value  $g_0$  in finite systems.

We might expect the irrelevant length scale  $\zeta$  to be less important as the localization length  $\xi$  increases and dominates when the band center ( $E_c = 0$ ) is approached. On the other hand, the irrelevant variable clearly affects our results in the tails where  $\xi$  is small. The width of the Thouless number defined by Eq. (11), however, depends strongly on the



**Figure 4.** The localization length critical exponent  $\nu$  in the second lowest subband, calculated for different correlation length  $l$  of the random potential, from the scaling of the area  $A(L)$  with size,  $L$ . The inset shows the area  $A(L)$  of Thouless number  $g(E)$  of the second lowest subband as a function of size  $L$  on a log-log scale.

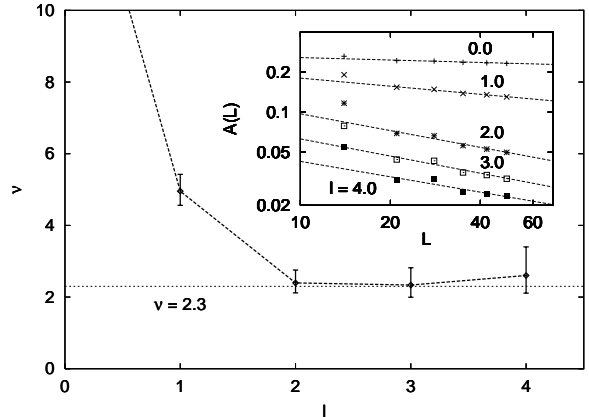
scaling behaviour of the tail, since the value of  $g(E)$  in the tails is amplified by multiplying  $(E - E_c)^2$  in the numerator. Therefore, the localization length exponent obtained from the finite-size scaling of the area  $A(L)$  of the Thouless number may be more reliable (which includes the finite-size effect of the peak conductance as well).

Figure 4 inset shows the area of Thouless number  $g(E)$  of the second lowest subband as a function of size  $L$ . On the log-log plot, the area  $A(L)$  versus  $L$  follows straight lines with different slopes. The numerical value of the localization length critical exponent  $\nu$  calculated based on Eq. (14) is summarized in Fig. 4. The universal value  $\nu = 2.2 \pm 0.2$  is restored for  $l \geq 1$ . These values of  $l$  are consistent with the observation in Fig. 3 that  $W(L)$  is minimized with  $l = 2$ .  $\nu = 6.5$  with  $l = 0$  is, again, due to the finite size effects as a result of the large localization length.

### 4.3 The third lowest subband

In even higher subbands (Landau levels), the localization length  $\xi$  is expected to be even larger than  $\xi$  in the second subband, with both uncorrelated and correlated potential. We confirmed, in our calculations, that the effects of Gaussian correlated potential on the scaling behaviour of the third lowest (side) subband of the seven-subband system agree qualitatively with that of the second lowest subband. Once again, to minimize the effect of the irrelevant length scale  $\zeta$ , we plot the area  $A(L)$  of the Thouless number curve versus the system size  $L$  in the inset of Fig. 5. For  $L \geq 21$ ,  $A(L)$  follows straight lines on double logarithmic plot. Figure 5 summarizes the localization length critical exponent  $\nu$  calculated according to Eq. (14).  $\nu$  decreases from 16 with  $l = 0$  to  $\nu \simeq 2.3$  with  $l \geq 2$ . The  $\nu$  versus  $l$  curve is very similar to the curve in Fig. 4, except that, in the second subband,  $\nu$  is smaller with  $l = 0$ , and drops to  $\nu \simeq 2.3$  with  $l = 1$ . This is consistent with the fact that the localization length  $\xi$  is smaller in lower subband.

Therefore, due to rapidly increasing localization length in higher Landau levels and the



**Figure 5.** The localization length critical exponent  $\nu$  calculated at different correlation length  $l$ . The inset shows the area of Thouless number  $g(E)$  of the third lowest subband as a function of size  $L$  on a log-log scale.

consequent mesoscopic effects, finite size scaling of the area  $A$  under the Thouless number curves seems to be more reliable than the width of the Thouless number curve. A universal exponent  $\nu \simeq 2.3$  can be observed for correlated potential with certain correlation length in finite size samples. It is worth emphasizing that the universality, including localization length exponent and critical conductance, should be observed in large enough samples. These are beyond our current computing capabilities, but should become more accessible as computers get more powerful.

### 5. Quantum Hall Transitions in Multiple Subbands

In this section, we briefly present our results for multiple subbands. More details can be found elsewhere [1]. In a lattice with  $\phi/\phi_0 = 1/7$ , we projected the Hamiltonian to the lowest three subbands, carrying a total Hall conductance of  $3e^2/h$ . We found that, with increasing disorder, Thouless number  $g(n)$ , calculated as a function of filling factor  $n$ , evolves from three peaks separated by gaps at integer fillings to a smooth curve with no dips. Meanwhile, the plateaus of Hall conductance  $\sigma_{xy}$  at integer fillings, characteristic of quantum Hall transitions, disappears.

Figure 6 shows  $g(n)$  and  $\sigma_{xy}(n)$  as a function of filling  $n$ , with disorder strength  $W/t = 4.5$ , which corresponds to the strong disorder (weak field) limit. We calculated  $g(n)$  in a  $28 \times 28$  lattice, and  $\sigma_{xy}(n)$  in a  $14 \times 14$  lattice. The dip in  $g(n)$  near the upper end of the spectrum is affected by the truncation of higher subbands. However, at the lower end, we believe our data shows the correct low-field physics, since the energy levels in the subbands not included in the truncated model interact only weakly with the low-lying energy levels. For  $n \leq 1.5$ , we find that  $g(n)$  can be fit by a straight line, while the Hall conductance  $\sigma_{xy}$  is much smaller than the diagonal conductance, and is essentially zero. Such observations are generically available for systems of different magnetic flux and number of subbands.

We attribute our results to the “classical” behaviour of the two-dimensional electron gas. The linear dependence of the longitudinal conductance on electron concentration is

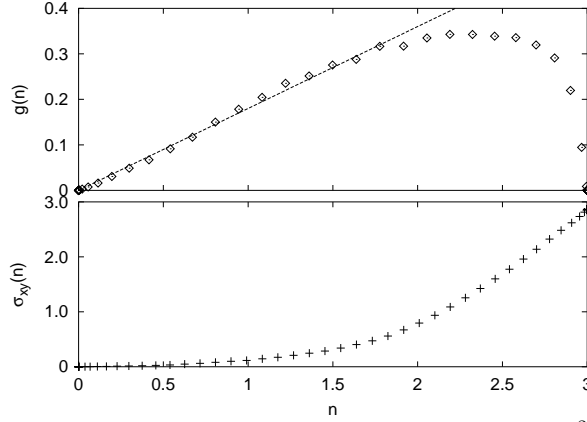


**Figure 6.** Thouless number and Hall conductance (in units of  $e^2/h$ ) in the truncated, three lowest subbands with  $W/t = 4.5$ .

consistent with the classical Drude conductivity  $\sigma_{xx} \sim n$ . This result seems to suggest that for finite sizes, due to the presence of long length scales, quantum interference effects can be cut off at strong disorder, or equivalently at weak magnetic field. This could explain the experimental phase diagram []. The concurrent vanishing  $\sigma_{xy}$  (lower panel of Figure 6) supports this scenario too. For further details, the reader is referred to Ref. [].

## 6. Conclusions

In summary, we have studied a tight-binding lattice model for non-interacting electrons, using projection to enable truncation of the Hilbert space to different combinations of the magnetic subbands. In a single magnetic (side) subband, we obtained, through finite-size scaling of Thouless number, the critical exponent  $\nu$  of the localization length  $\xi \sim |E - E_c|^{-\nu}$ , as  $\nu = 2.4 \pm 0.1$ , in good agreement with previous numerical results in continuum lowest Landau level model. The localization length critical exponent is universal, regardless of the strength and distribution of the random potential or magnetic field. In higher Landau levels, however, the rapidly increasing length scales can alter the scaling behaviour in finite size systems, a manifestation of mesoscopic effects in the quantum Hall regime. With the introduction of correlated potential, we demonstrated that the localization length can be reduced, leading to universal scaling behaviour of appropriately chosen quantities.

In a truncated system involving multiple magnetic side subbands (corresponding to multiple Landau levels), we found that the Hall conductance  $\sigma_{xy}$  of finite lattices evolves from a series of well-defined plateaus at  $ne^2/h$  for various integer Landau level filling to a single sharp rise at the upper end of the energy spectrum. At the same time, the Thouless number of the (finite) system become linear in filling factor  $n$ . The linear dependence is interpreted as a crossover to the classical (unquantized) Hall response, as the system size becomes comparable to, or smaller than, the very (exponentially) large localization lengths of the electronic eigenstates in this limit. While the sizes studied here are considerably smaller than those corresponding to experimental samples, our findings raise the question

of the proper interpretation of the experimentally observed low field transition, and the possibility of the influence of a quantum-classical crossover in experiments.

## 7. Acknowledgments

It is a pleasure to participate in the commemorative symposium (and its proceedings) in honor of Professor Narendra Kumar, who has made many significant contributions to the field of disordered and mesoscopic systems. This research was funded by NSF DMR-9809483.

## References

- [1] D. E. Khmel'nitskii, Phys. Lett. **106**, 182 (1984).
- [2] R. B. Laughlin, Phys. Rev. Lett. **52**, 2304 (1984).
- [3] S. Kivelson, D. H. Lee, and S. C. Zhang, Phys. Rev. B **46**, 2223 (1992).
- [4] H. W. Jiang, C. E. Johnson, K. L. Wang, and S. T. Hannahs, Phys. Rev. Lett. **71**, 1439 (1993).
- [5] R. J. F. Hughes *et al.*, J. Phys. Condens. Matter **6**, 4763 (1994).
- [6] T. Wang *et al.*, Phys. Rev. Lett. **72**, 709 (1994).
- [7] S. H. Song *et al.*, Phys. Rev. Lett. **78**, 2200 (1997).
- [8] M. Hilke *et al.*, Phys. Rev. B **62**, 6940 (2000).
- [9] S. V. Kravchenko, W. Mason, J. E. Furneaux, and V. M. Pudalov, Phys. Rev. Lett. **75**, 910 (1995).
- [10] D. N. Sheng and Z. Y. Weng, Phys. Rev. B **62**, 15363 (2000).
- [11] D. N. Sheng, Z. Y. Weng, and X. G. Wen, cond-mat/0003117 (unpublished).
- [12] D. Hofstadter, Phys. Rev. B **14**, 2239 (1976).
- [13] D. J. Thouless, M. Kohmoto, M. P. Nightingale, and M. den Nijs, Phys. Rev. Lett. **49**, 405 (1982).
- [14] Q. Niu, D. J. Thouless, and Y. S. Wu, Phys. Rev. B **31**, 3372 (1985).
- [15] Y. Huo and R. N. Bhatt, Phys. Rev. Lett. **68**, 1375 (1992).
- [16] K. Yang and R. N. Bhatt, Phys. Rev. Lett. **76**, 1316 (1996).
- [17] D. N. Sheng and Z. Y. Weng, Phys. Rev. Lett. **80**, 580 (1998).
- [18] Y. Huo, *Numerical Studies in the Lowest Landau Level*, Ph.D. thesis, Princeton University, 1994.
- [19] D. P. Arovas *et al.*, Phys. Rev. Lett. **60**, 619 (1988).
- [20] J. T. Edwards and D. J. Thouless, J. Phys. C **5**, 807 (1972).
- [21] D. C. Licciardello and D. J. Thouless, J. Phys. C **8**, 4157 (1975).
- [22] R. N. Bhatt, in *Physical Phenomena at High Magnetic Fields*, edited by E. Manousakis *et al.* (Addison-Wesley, Reading, 1991), p. 65.
- [23] B. Huckestein, Rev. Mod. Phys. **67**, 357 (1995).
- [24] D. Z. Liu and S. D. Sarma, Phys. Rev. B **49**, 2677 (1994).
- [25] J. T. Chalker and P. D. Coddington, J. Phys. C **21**, 2665 (1988).
- [26] M. Guo and R. N. Bhatt, unpublished.
- [27] H. Aoki and T. Ando, Phys. Rev. Lett. **54**, 831 (1985).
- [28] T. Ando and H. Aoki, J. Phys. Soc. Jpn. **54**, 2238 (1985).
- [29] B. Mielck, Europhysics Lett. **13**, 453 (1990).
- [30] B. Mielck, Z. Phys. B **90**, 427 (1993).
- [31] B. Huckestein, Europhysics Lett. **20**, 451 (1992).

- [32] X. Wan, *A Study of Quantum Phase Transitions in Two Dimensional Electron Systems*, Ph.D. thesis, Princeton University, 2000.
- [33] X. Wan and R. Bhatt, to be published.
- [34] X. Wan and R. N. Bhatt, cond-mat/0104281 (to appear in Phys. Rev. B).